2-D Direction-of-Arrival Estimation System Using Circular Array With Mutually Coupled Reference Signal

Michael Nazaroff, Gangil Byun, *Member, IEEE*, Hosung Choo, *Senior Member, IEEE*, Junghoon Shin, and Youngwook Kim, *Senior Member, IEEE*

***Abstract*— Direction-of-arrival (DOA) systems rely on proper phase measurements acquired from receiving antennas for optimal performance. Unfortunately, imperfections in any antenna and receiver system may present false phase measurements, the major cause of DOA estimation error. This paper discusses experimental results from an actual implementation of synchronizing a DOA circular array receiver system to mitigate these imperfections. A reference signal located at the center of the DOA array was coupled to array elements such that both the coupled reference signals and signals from a target were captured simultaneously in the receiver. This coupled reference signal was used to compensate for any phase error offsets produced by receiver system imperfections on cable length, phase of local oscillators, and phase delays in active devices. Furthermore, this approach did not necessitate an off-line calibration process of each receiver channel requiring accurate measurements. We implemented a 16-element circular array DOA estimation system using the Universal Software Radio Peripheral platform operating in the *S*- and *C*-bands. Results show that this implementation was able to combat receiver phase offset errors and estimated the DOA angles with an rms error of 0.92°.**

***Index Terms*— DOA estimation, multiband DOA, MUSIC, synchronization, software-defined radio.**

I. Introduction

DIRECTION of Arrival (DOA) estimation has been a topic of interest for several decades due to its many applications in defense and civil areas. Radar systems that localize targets have been used for DOA estimation [1]–[3]. Recently DOA estimation has also found applications in smart antenna systems [4], [5]. A smart antenna system placed at a wireless base station uses DOA estimation to localize a wireless user that it is serving. The base station performs dynamic beamforming to offer better quality of service toward the user after estimating its location. Fundamentally, DOA systems employ an antenna array upon which a signal emitted from a target impinges. A target location relative to each antenna element is represented by the phase of the signals being received at each array channel. Signal processing techniques such as Bartlett, minimum variance distortionless response (MVDR), multiple signal classification (MUSIC), estimation of signal parameters via rotational invariant techniques (ESPRIT), and others [6], [7] have been intensively applied to phase-delayed samples from each antenna to estimate the DOA of a target for various applications.

DOA estimation is sensitive to phase errors due to its dependence on the array phase pattern. Practicable systems present imperfections that would result in significant measurement errors in phase. Such imperfections can come from manufacturing errors of antennas, mutual coupling between array elements, differences in RF cable characteristics, and inconsistency in circuit parameters [8]. In addition, timing phase errors in multiple receivers of the array system should be considered. The received signal experiences a phase error if the phases of the shared LO and the clock of an A/D converter of each receiver are not synchronized. Many efforts have attempted to remedy these imperfections so that measured phase errors can be reduced. Most of these methods involve offline calibration to compensate for phase errors that cause the actual steering vector to deviate from a steering vector under ideal conditions [9]. The offline method of calibration is traditional, but may be undesirable in that it cannot be adaptive to time-varying characteristics of the array and receiver caused by mechanical vibration, temperature change, and system degradation.

Methods have been proposed where the calibration process is incorporated using an automated online approach that assumes time-varying array characteristics. One proposed method mutually coupled a reference signal originating from an antenna at the center of a uniform circular array [10]. This method was simulated and its results demonstrated the effectiveness of coupling a reference signal to measure gain and phase errors of a uniform circular array for calibration purposes. A similar method was conducted experimentally using an actual uniform linear array with a nearby antenna providing the coupled reference signal [11]. To the best knowledge of the authors of this presented paper, an online phase compensation system using a reference signal for a circular array has not been implemented.

Manuscript received July 1, 2018; revised August 23, 2018; accepted September 2, 2018. Date of publication September 20, 2018; date of current version November 13, 2018. The associate editor coordinating the review of this paper and approving it for publication was Prof. Kazuaki Sawada. *(Corresponding author: Youngwook Kim.)*

M. Nazaroff and Y. Kim are with the Department of Electrical and Computer Engineering, California State University, Fresno, CA 93740 USA (e-mail: youngkim@csufresno.edu).

G. Byun is with the Department of Electrical and Computer Engineering, Ulsan National Institute of Science and Technology, Ulsan 44919, South Korea.

H. Choo is with the Department of Electrical and Computer Engineering, Hongik University, Seoul 04066, South Korea.

J. Shin is with the Agency for Defense Development, Daejeon 34186, South Korea.

Digital Object Identifier 10.1109/JSEN.2018.2871464

In this paper, we designed a 16-element uniform circular array with a reference antenna for online calibration during DOA operation. The transmitter/receiver system was implemented using the universal software defined radio platform (USRP). A sinusoidal reference signal located at the center of a circular antenna array was mutually coupled to all array antennas. Each antenna simultaneously captured both the coupled reference signal and signals from a target. Therefore, the phase of a signal from a target became fixed relative to the reference signal. Even though each channel experienced a different phase delay, the actual phase of the signal from the target could be reconstructed after compensating for the phase error that can be found by use of the reference signal. This approach was capable of conducting real-time array phase error correction without requiring any measurement of an error matrix. A 16-element circular array operating at C band was designed for the estimation of 2D DOA. Multiple software-defined radios were used for the receiver system. Finally, we applied the MUSIC and multi-tone DOA estimation algorithms to verify our system. We used a single tone, multi-tones, and a frequency modulated continuous wave as a source. The performance of the circular array system was tested in an anechoic chamber. The circular array design, hardware system design, DOA estimation algorithm, measurements, and the results are discussed in this paper.

II. Design of 16-Element Circular Array

We designed a 16-element circular array using microstrip patch antennas for the two-dimensional DOA estimation. The constructed array consisted of 16 identical patch antennas arranged with a uniform angular separation of 22.5° and a reference antenna located at the center. Each antenna had a polygon shape radially formed with respect to the patch center, which included triangular, rectangular, elliptical, and even circular shapes. In our approach, radii to the polygon vertices were adjusted to generically investigate the most appropriate design near the edge of a finite substrate. The substrate used in our approach was FR4 with a thickness of 1.6 mm, having dielectric properties of $\varepsilon_r = 4.5$ and $\tan\delta = 0.02$. Note that the radiation pattern of an antenna near the substrate edge tended to collapse toward outside of the substrate, and this became more significant in the presence of mutual coupling between antennas. For the reference antenna, we implemented a conventional quarter-wavelength monopole owing to its omnidirectional radiation pattern. As the distance from the reference monopole to each patch antenna was the same, the phase of reference signal received from each patch was identical. Therefore, the reference signal could be used in the phase compensation for each channel.

Fig. 1 shows a fabricated array optimized to operate at 2.5 GHz. As can be seen, the shape of each patch is similar to an ellipse that is diagonally rotated with a maximum width (w_{max}) of 52.6 mm (0.43λ at 2.5 GHz). The radius of the circular array is 200 mm (1.6λ), and the inter-element spacing between the radiating elements is 75 mm (0.6λ). The diameter of the ground platform is 500 mm, corresponding to 4.1λ, and the substrate within the inner circle is carved out in the fabricated circular array to lower the unnecessary payload.

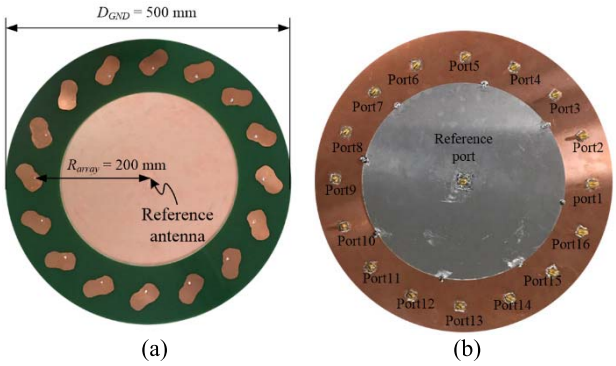

Fig. 1. Fabricated 16-element circular array with center reference antenna: (a) front of the circular array; (b) back of the circular array.

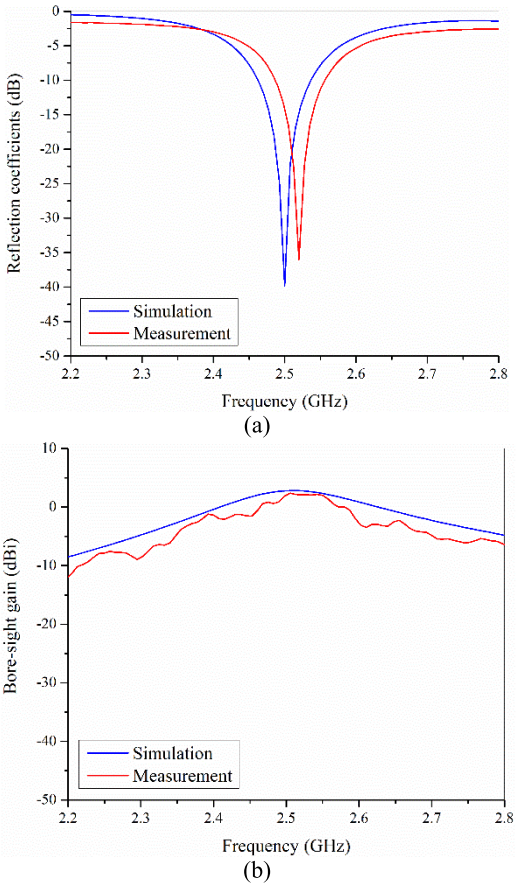

Fig. 2. Comparisons of measured and simulated antenna characteristics at Port 1: (a) reflection coefficients; (b) bore-sight gain.

Fig. 2 presents comparisons of reflection coefficients and bore-sight gains as a function of frequency. The antenna is well matched at 2.5 GHz with measured and simulated reflection coefficients of −36 dB and −39.8 dB, respectively. The simulated bore-sight gain is 2.8 dBi and is similar to the measured value of 2.4 dBi. Fig. 3 shows radiation patterns of Ant. 1 (Port 1) at 2.5 GHz. There is no significant pattern distortion in the upper hemisphere with measured half-power beamwidths (HPBWs) of 79.8° in the z-x plane and 93° in the y-z plane. Measured gain deviations in the upper hemisphere are 13 dB and 11.8 dB in the z-x and y-z planes, respectively.

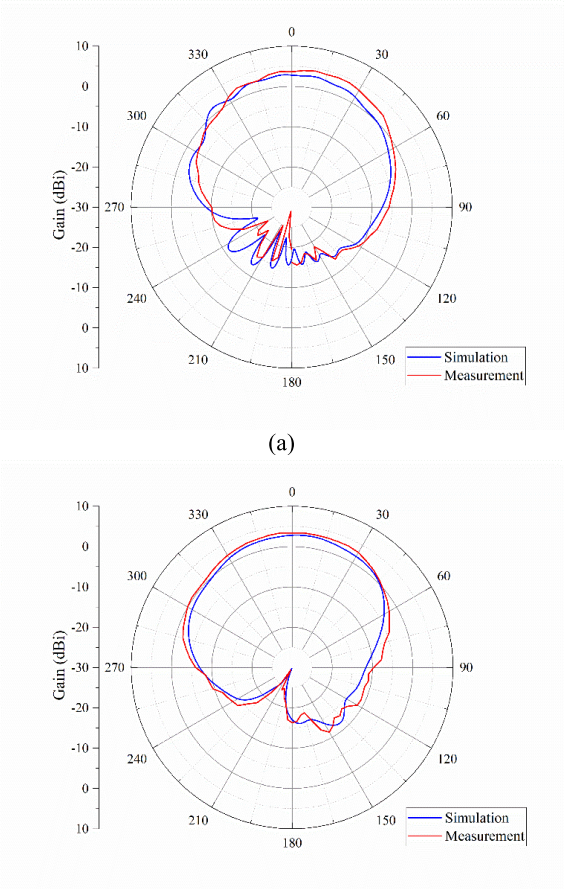

Fig. 3. Comparisons of measured and simulated radiation patterns at Port 1: (a) z-x plane; (b) z-y plane.

III. System Implementation

Hardware implementation in this study consisted of USRPs from National Instruments (NI). The URSP could interface with a host computer where code could be written for a custom wireless communication application. Such customizability included setting up the USRP from using a particular carrier frequency and channel gain to sending a designed signal and processing received signals. Quadrature mixer was used by the USRP where baseband samples were sent from the host computer for transmission and received signals were down-converted and sent to the host computer during reception. We used NI-2943R as USRP. The operating frequency of the USRP was from 2 GHz to 6 GHz, and the bandwidth was 120 MHz. The baseband sampling rate varied depending on the data transmission speed to the host computer. We used maximum 100Msps.

For the transmitter, we used a single NI-2943R, connecting a horn antenna. The USRP could modulate any random shape of baseband wave with an RF carrier frequency and transmit it. Because the USRP had two transmitting channels, code was written in LabVIEW to send out two separate signals. One channel served as the actual Tx message signal that was regarded as a signal from a target. The other transmitting channel was connected directly to the reference antenna at

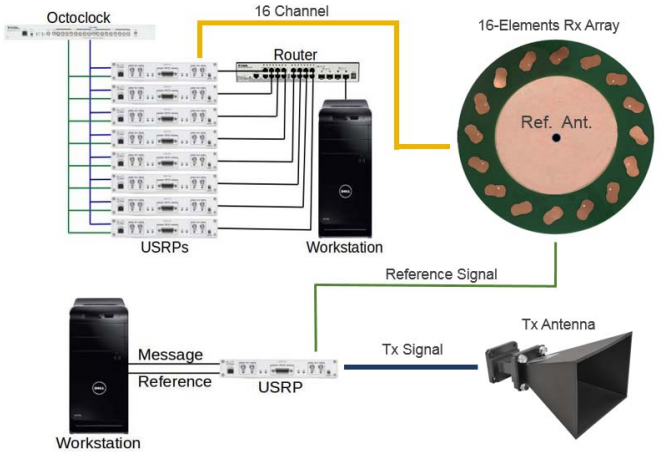

Fig. 4. Tx and Rx system diagram with USRPs and circular array antenna.

the array center using a cable to provide the reference signal. The reference signal was a sinusoidal wave.

The receiver system used eight USRPs. Each USRP had a dual-receiver channel, yielding 16 channels. Each individual array element in the 16-element circular array was allocated its own dedicated USRP channel. The eight USRPs were connected with an Ethernet router that was also connected to a host computer. A GNURadio programming framework was used to configure the receiver USRPs and download data from each channel. Data were saved in the host computer and were processed by Matlab in real time.

All radios shared the same LO and external clock (PPS signal in USRP operation), which provided hardware synchronization to make the sampling time identical in each channel. We used an Octoclock from NI to provide the external clock and LO. However, this circuit did not achieve full synchronization as the timing error was a couple of micro-seconds in practice. The micro-second error was critical and caused large phase errors that deteriorated DOA estimation accuracy. To achieve correct DOA estimation, we needed the sampling timing error to fall within the range of a few pico-seconds. Fortunately, it was also possible to compensate for the timing error by the use of a reference signal. Fig. 4 shows a diagram of the transmitter and receiver system. Algorithms built upon MUSIC and ISSM were used for the DOA estimation.

IV. Phase Compensation

Based on the proposed scheme, each channel could be calibrated through the reference signal. Since all array elements were equidistant from the reference antenna, no phase differences of the measured reference signal would be expected between the antennas. However, the measured reference signal at each element experienced a different phase due to the system imperfections in antenna manufacturing, cable length, phase of local oscillators, phase delays in active devices, and sampling timing for examples. Among them, the sampling timing is the most significant component that causes the phase error. Since the phase delays experienced for the reference signal and the received message signal at each channel should be same, the reference signal could be used to compensate

for the phase of the target signal. This was achieved by selecting a certain array element that would serve as the zero-phase baseline for the other antennas. GNURadio was used to acquire samples from the 16 receiving radios simultaneously. From these samples, the reference signal was extracted, and the corresponding phases were detected through a fast Fourier transform (FFT). Then, each channel was phase-compensated by Matlab in real time. The calibrated message phase for the *m-th* channel is acquired from

$$\varphi_{m,cal} = (\varphi_m - \varphi_0) - \alpha_{ref}(\varphi_{ref,m} - \varphi_{ref,0}) \tag{1}$$

where φ_m and φ_0 are the uncalibrated DOA target signal phases acquired by the *m-th* and first array element. Terms $\varphi_{ref,m}$ and $\varphi_{ref,0}$ are the reference signal phases measured at the *m-th* and first elements. The term α_{ref} is a scaling factor computed from

$$\alpha_{ref} = \frac{f_{msg} + f_c}{f_{ref} + f_c} \tag{2}$$

where f_{msg} is a frequency term contained in the DOA target signal, f_{ref} is the frequency of the reference signal, and f_c is the operating carrier frequency. The target signal may be composed of one or more frequencies.

V. DOA Estimation Algorithms

A. Signal Model

DOA estimation relies on the physical arrangement of an array antennas. This can be a uniform linear arrangement for 1D DOA estimation, or a circular array for 2D estimation in general. The physical angle of the target's location translates to each antenna perceiving a particular phase of the signal being transmitted by this target [12]. In a linear array, the phase delay is linearly proportional to an element's position. In contrast, the phase pattern is complex for a circular array. A single target of interest is assumed to be located with elevation and azimuth angles θ and ϕ relative to the array.

The electromagnetic wave front of the signal emitted from the target travels different distances to each element. Assuming a circular array of M elements, signals acquired by each element can be compactly expressed as the following narrowband model:

$$\mathbf{x}(t) = \left[A_0 e^{-\mathrm{j}(2\pi f_c t + \alpha_0)} \dots A_{M-1} e^{-\mathrm{j}(2\pi f_c t + \alpha_{M-1})}\right] \tag{3}$$

In (3), the indexing from *0* to $M-1$ traverses from the first element to the last element. The term $e^{-\mathrm{j}2\pi f_c t}$ models the signal originating from the target. In standard DOA processing, an array element is designated as the reference with a zero degree phase shift. Phases of all other elements are measured in relation to this reference element. Since the system is only working with single-tone narrowband signals, frequency terms can be disregarded when analyzing phase. Also, terms depicting amplitude may also be disregarded because amplitude does not have DOA information when the target is in a far field. This results in the array steering vector. A steering vector for a 2-dimensional DOA application using a circular array can be written as

$$\mathbf{a}(\theta, \phi) = \left[e^{-\mathrm{j}\frac{2\pi}{\lambda_c}\tau_0} \dots e^{-\mathrm{j}\frac{2\pi}{\lambda_c}\tau_m} \dots e^{-\mathrm{j}\frac{2\pi}{\lambda_c}\tau_{M-1}}\right] \tag{4}$$

The steering vector presents a relationship between the DOA angle of the target and phase measurements between array elements. The term τ_m is written in terms of the coordinates (x_m, y_m, z_m) of the *m-th* antenna relative to the array center and the target location (θ, ϕ) as

$$\tau_m = -x_m \sin(\theta)\cos(\phi) - y_m \sin(\theta)\sin(\phi) - z_m \cos(\theta) \tag{5}$$

A vector $\mathbf{x}(t)$ compactly representing signals acquired at each antenna can be written in terms of the steering vector and a scalar $s(t)$ representing the signal originating from the target in the following way:

$$\mathbf{x}(\mathrm{t}) = \mathbf{a}(\theta, \phi)\mathbf{s}(\mathrm{t}) + \mathbf{n}(\mathrm{t}) \tag{6}$$

Vector $\mathbf{n}(\mathrm{t})$ models noise present at the *m-th* antenna. If there are D targets of interest, then

$$\mathbf{x}(\mathrm{t}) = \mathbf{A}(\theta, \phi)\mathbf{s}(\mathrm{t}) + \mathbf{n}(\mathrm{t}) \tag{7}$$

Matrix $\mathbf{A}(\theta, \phi)$ from (7) is a steering matrix whose columns are the array steering vectors for each different target. This is a more general model for any given number of D targets, instead of a model restricted to a single target.

B. MUSIC

The MUSIC algorithm is a subspace method that can be used for estimating DOA angles using narrowband signals [13]. This approach starts by creating an autocorreleation matrix of the samples acquired from the array elements. Eigenvalue decomposition is applied to this autocorreleation matrix from which a set of vectors span the signal subspace, and the rest represents the noise subspace. These two subspaces are orthogonal to each other. Let $\hat{\mathbf{V}}$ contain the eigenvectors spanning the noise subspace. Then, MUSIC uses this orthogonality to create the following pseudospectrum:

$$P_{MUSIC}(\phi) = \frac{1}{\mathbf{a}(\phi)^H \hat{\mathbf{V}} \hat{\mathbf{V}}^H \mathbf{a}(\phi)} \tag{8}$$

The product in the denominator will become zero when the parameter ϕ happens to be the DOA angle of the target whence the measured signal originated. This would result in peaks in the pseudospectrum depicting the angular location of the target.

C. Multiple Frequency DOA Estimation

The signal models presented by (3) assume a narrowband signal. However, there are scenarios where a signal being received may be composed of multiple frequency components. The use of multiple frequencies can improve the DOA estimation result instead of narrowband methods that use information from a single frequency point. DOA methods have been developed to process signals composed of multiple frequency components, such as the incoherent signal subspace method (ISSM) [14], coherent signal subspace method (CSSM) [15], and WAVES [16]. DOA algorithms that were employed in this study for working with multiple frequency signals analyzed data collected from an array at discrete

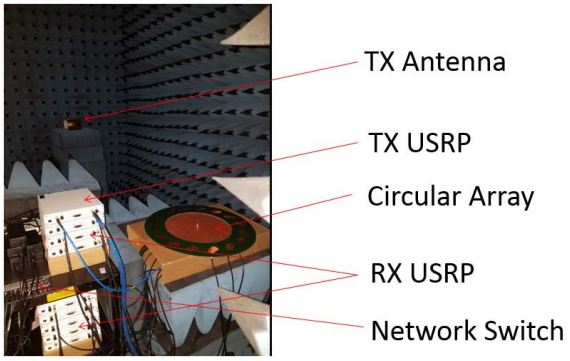

Fig. 5. DOA measurement setup in an anechoic chamber.

frequency bins. This can be expressed for a 2D array by taking the discrete Fourier transform (DFT) of (7) to obtain

$$\mathbf{X}(f_i) = \mathbf{A}(f_i, \theta, \phi)\mathbf{S}(f_i) + \mathbf{N}(f_i) \tag{9}$$

where f_i denotes the frequency bin of analysis. A received DOA signal may have its spectral content contained within B frequency bins. FFT-based peak detection would determine the B frequency bins that contain the spectral content of the received DOA message. The calibrated phase expressed by (1) would then be calculated for the *b-th* frequency bin for all M array elements. This process is repeated over all B frequency bins containing the DOA message spectral content to obtain the following $M \times B$ matrix

$$\varphi_{cal} = \begin{bmatrix} \varphi_{0,cal} & \cdots & \varphi_{B-1,cal} \end{bmatrix} \tag{10}$$

where $\varphi_{b,cal}$ is a vector that contains the compensated DOA message phases of the *b-th* frequency bin for all M array elements. Computation of these B phases is repeated over J time windows of data size N_{win}. Results computed from each time window were appended to create a single $M \times J \cdot B$ matrix Φ_{cal}. An autocorrelation matrix is computed on Φ_{cal} as

$$\mathbf{R}_{\Phi_{cal}\Phi_{cal}} = E\left[\Phi_{cal}\Phi_{cal}^H\right] \tag{11}$$

This process takes the DOA signal content from multiple frequency bins and creates a single autocorreleation matrix. Eigenvalue decomposition is then applied to this autocorrelation matrix to generate eigenvectors for the signal and noise subspaces. The resulting noise eigenvectors are then used as $\hat{\mathbf{V}}$ in (8) for the MUSIC DOA estimation.

VI. Experimental Results

Our implemented 2D DOA system was tested in an anechoic chamber located at California State University, Fresno. Both transmitting and receiving radios were tuned to a 2.45 GHz carrier. A 500 kHz single-tone sinusoidal served as the reference signal, while the transmitted message signal transmitted varied among a single tone, multi-tone, and frequency modulated continuous wave (FMCW). The measurement setup is shown in Fig. 5.

The first test involved varying the target location relative to the receiving array along azimuth direction. We used a 2451 MHz target message signal (1 MHz single tone), transmitted from the Tx antenna. Data collected was processed both with and without the phase compensation using the reference signal. Comparison results are shown in Table 1. The error experienced with the reference signal seems stable, with no erratic fluctuations across different angles, unlike measurements taken without the reference signal. The average DOA estimation error was near 0 degrees. A second test was performed using the same setup as the first, except that the elevation of the Tx antenna was varied. Shown in Table 2 are results of this test, compared to processing without reference signal compensation. Results of using the reference signal have a higher DOA estimation accuracy than those without

TABLE I

Azimuth Direction of Arrival Measurements With Reference Signal Correction

Actual DOA (degrees)	*Estimated DOA without Compensation (degrees)*	*Estimated DOA with Compensation (degrees)*
-45.0	-39.9	-44.2
-22.5	49.1	-23.2
0	26.1	0.8
22.5	48.1	22.8
45.0	-2.9	43.8

TABLE II

Elevation Direction of Arrival Measurements With Reference Signal Correction

Actual DOA (degrees)	*Estimated DOA without Compensation (degrees)*	*Estimated DOA with Compensation (degrees)*
46	46.4	44.3
59	4.40	59.2
75	42.4	75.7
89	79.7	90.0

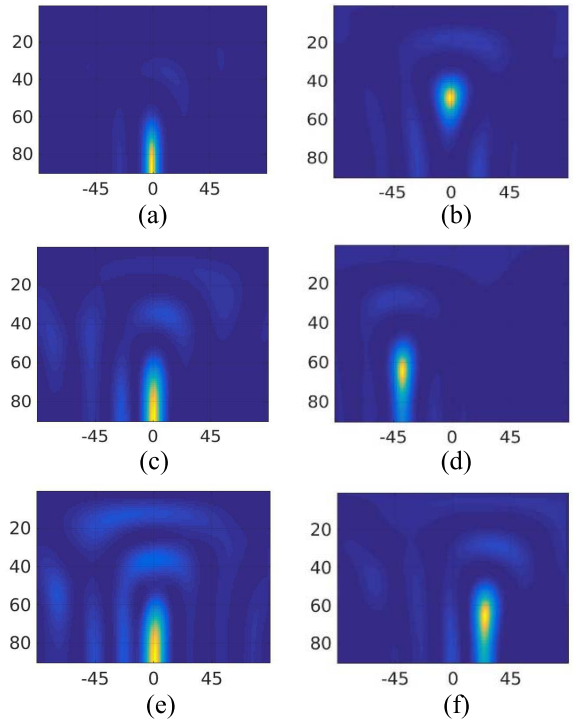

Fig. 6. (a), (b) DOA result using a single-tone; (c), (d) DOA results usng multiple tones as target message; (e), (f) DOA results using FMCW as target message.

the reference signal. Estimation performance suffered as the target was elevated beyond 60° from the base of the array. This was due to ambiguity in resolving DOA angles as the Tx antenna moved close to $\theta = 90°$ relative to the array using spherical coordinates. The average root mean squire (RMS) error from the two tests was 0.92 degrees.

Transmitted target messages created from multiple frequencies were also used to test the ISSM of the DOA system. Messages were varied in three separate tests. A single 2 MHz message was used in the first test. In the second test, 5 MHz, 10 MHz, 15 MHz, 20 MHz, and 25 MHz tones were used as the message. During the third test, a 5 MHz to 25 MHz chirp signal with a 20 μs ramp time served as the message. Fig. 6 shows the results of these tests when the target was situated relative to the DOA array with azimuth angles at 0 degrees and elevation angles at 90 degrees. The DOA could be estimated with the same level of accuracy as in the case of using a single tone for the target message signal. Also shown in Fig. 6 are DOA estimations when the target was varied at different positions. The target was positioned at $(\theta, \phi) = (0°, 45°)$ for the single-tone, $(\theta, \phi) = (-45°, 60°)$ for the multi-tone, and $(\theta, \phi) = (25°, 65°)$ for the FMCW signal.

VII. Conclusion

We proposed to reduce phase errors at each channel through the use of the reference signal mutually coupled to antenna array elements. We implemented a 2D DOA estimation system with a software-defined radio approach. Even though multiple software-defined radios use external clocking circuits for synchronizing every radio, the precision was not enough for the accuracy needed for DOA estimation. The proposed method of mutually coupling a reference signal to array elements can further mitigate phase errors that are still left over after applying external synchronization circuits. The approach presented in this paper does not rely upon manual calibration or lookup tables to compensate for phase errors. In addition, the calibrations can be done in real time whenever necessary during system operation. Therefore, these factors make it a flexible and robust strategy for implementing a DOA receiver system that is more resilient against phase errors. Furthermore, the experimental results demonstrate that this approach also yields satisfactory results in ISSM applications where a target signal is not simply a single-tone carrier.

References

[1] E. Fishler, A. Haimovich, R. Blum, L. Cimini, D. Chizhik, and R. Valenzuela, "MIMO radar: An idea whose time has come," in *Proc. IEEE Int. Radar Conf.*, Philadelphia, PA, USA, Apr. 2004, pp. 71–78.

[2] D. Oh, Y. Ju, H. Nam, and J.-H. Lee, "Dual smoothing DOA estimation of two-channel FMCW radar," *IEEE Trans. Aerosp. Electron. Syst.*, vol. 52, no. 2, pp. 904–917, Apr. 2016.

[3] X. F. Zhang, L. Y. Xu, L. Xu, and D. Z. Xu, "Direction of departure (DOD) and direction of arrival (DOA) estimation in MIMO radar with reduced-dimension MUSIC," *IEEE Commun. Lett.*, vol. 14, no. 12, pp. 1161–1163, Dec. 2010.

[4] M. Pastorino and A. Randazzo, "A smart antenna system for direction of arrival estimation based on a support vector regression," *IEEE Trans. Antennas Propag.*, vol. 53, no. 7, pp. 2161–2168, Jul. 2005.

[5] D. M. Vijayan and S. K. Menon, "Direction of arrival estimation in smart antenna for marine communication," in *Proc. Int. Conf. Commun. Signal Process.*, Melmaruvathur, India, Apr. 2016, pp. 1535–1540.

[6] P. L. Shrestha, M. Hempel, P. Mahasukhon, T. Ma, and H. Sharif, "Performance analysis for direction of arrival estimating algorithms," in *Proc. 75th Veh. Tech. Conf.*, Yokohama, Japan, May 2012, pp. 1–5.

[7] Z. Chen and G. K. Gokeda, "Overview of basic DOA estimation algorithms," in *Introduction to Direction-Of-Arrival Estimation*, 1st ed. Norwood, MA, USA: Artech House, 2010, ch. 3, pp. 31–64.

[8] M. Eberhardt, P. Eschlwech, and E. Biebl, "Investigations on antenna array calibration algorithms for direction-of-arrival estimation," *Adv. Radio Sci.*, vol. 14, pp. 181–190, Sep. 2016.

[9] K. R. Dandekar, H. Ling, and G. Xu, "Smart antenna array calibration procedure including amplitude and phase mismatch and mutual coupling effects," in *Proc. IEEE Int. Conf. Pers. Wireless Commun.*, Hyderabad, India, Dec. 2000, pp. 293–297.

[10] T. Ouyang, L. Qian, L. Ding, and F. Yang, "Mutual coupling calibration for uniform circular array using a single source," in *Proc. 6th Int. Conf. Wireless Commun. Signal Process.*, Hefei, China, Oct. 2014, pp. 1–6.

[11] M. Wang, Z. Wang, and Z. Cheng, "Joint calibration of mutual coupling and channel gain/phase inconsistency using a near-field auxiliary source," in *Proc. 13th Int. Conf. Signal Process.*, Chengdu, China, Nov. 2016, pp. 394–398.

[12] M. Moody, "Direction of arrival estimation using a sparse circular array and multiplicative beamforming," *IEEE Trans. Antennas Propag.*, vol. AP-31, no. 4, pp. 678–682, Jul. 1983.

[13] P. Stoica and R. Moses, "Spatial methods," in *Spectral Analysis of Signals*, 1st ed. Upper Saddle River, NJ, USA: Prentice-Hall, 2005, ch. 6, pp. 263–327.

[14] G. Su and M. Morf, "The signal subspace approach for multiple wide-band emitter location," *IEEE Trans. Acoust., Speech, Signal Process.*, vol. ASSP-31, no. 6, pp. 1502–1522, Dec. 1983.

[15] H. Wang and M. Kaveh, "Coherent signal-subspace processing for the detection and estimation of angles of arrival of multiple wide-band sources," *IEEE Trans. Acoust., Speech, Signal Process.*, vol. ASSP-33, no. 4, pp. 823–831, Aug. 1985.

[16] E. D. di Claudio and R. Parisi, "WAVES: Weighted average of signal subspaces for robust wideband direction finding," *IEEE Trans. Signal Process.*, vol. 49, no. 10, pp. 2179–2191, Oct. 2001.

Michael Nazaroff received the B.S. degree in electrical engineering and the M.S. degree in engineering from California State University, Fresno, CA, USA, in 2012 and 2018, respectively. He is currently an Electrical Engineer in Fresno and a Research Assistant at California State University. His research interests include software-defined radio, wireless communication, and signal processing.

Gangil Byun (S'12–M'15) received the B.S. and M.S. degrees in electronic and electrical engineering from Hongik University, Seoul, South Korea, in 2010 and 2012, respectively, and the Ph.D. degree in electronics and computer engineering from Hanyang University, Seoul, in 2015. After his graduation, he returned to Hongik University to work as a Research Professor and performed active research for two years. He joined the Faculty of the Ulsan National Institute of Science and Technology in 2018, where he is currently an Assistant Professor of Electrical and Computer Engineering. His principal areas of research are in the design and analysis of small antenna arrays for adaptive beamforming applications, such as the direction of arrival estimation, interference mitigation, and radar. His recent research interests also include circularly-polarized antennas, vehicular and aeronautic antennas, global positioning system antennas, and antenna and array configuration optimization. He has actively contributed to the consideration of both antenna characteristics and signal processing perspectives for the improvement of overall beamforming performances.

Hosung Choo received the B.S. degree in radio science and engineering from Hanyang University, Seoul, South Korea, in 1998, and the M.S. and Ph.D. degrees in electrical and computer engineering from the University of Texas at Austin in 2000 and 2003, respectively. In 2003, he joined the School of Electronic and Electrical Engineering, Hongik University, Seoul, where he is currently a Professor. His principal area of research includes electrically small antennas for wireless communications, reader and tag antennas for RFID, on-glass and conformal antennas for vehicles and aircraft, and array antennas for GPS applications.

Junghoon Shin is at the Agency for Defense Development.

Youngwook Kim (S'03–M'08–SM'14) received the B.S. degree in electrical engineering from Seoul National University, South Korea, in 2003, the M.S. and Ph.D. degrees in electrical and computer engineering from the University of Texas at Austin, USA, in 2005 and 2008, respectively. He is currently a Professor with the Department of Electrical and Computer Engineering, California State University, Fresno. He has published more than 75 technical papers. His research interests are in the area of radar signal processing, antenna design, and RF electronics. His primary topic of research lies in radar target classification with machine-learning techniques. Currently, remote detection, monitoring and analysis of human motions using EM wave have been the focus in his research with deep learning algorithms. He was a recipient of the LCOE Outstanding Research Award, the Claude Laval Jr. Award, Provost's New Faculty Award from the California State University, the A.D. Hutchison Fellowship from the University of Texas at Austin, and the National IT Fellowship from the Ministry of Information and Communication, South Korea.